Nuclear Instruments and Methods in Physics Research A 765 (2014) 262–268

Contents lists available at ScienceDirect

Nuclear Instruments and Methods in Physics Research A

journal homepage: www.elsevier.com/locate/nima

Two-dimensional diced scintillator array for innovative, fine-resolution gamma camera

T. Fujita [a,*], J. Kataoka [a], T. Nishiyama [a], S. Ohsuka [b], S. Nakamura [c], S. Yamamoto [d]

[a] Research Institute for Science and Engineering, Waseda University, Shinjuku, Tokyo 169-8555, Japan
[b] Central Research Laboratory, Hamamatsu Photonics K.K., 5000, Hirakuchi, Hamakita-ku, Hamamatsu, Shizuoka, Japan
[c] Solid State Division, Hamamatsu Photonics K.K., 1126-1, Ichino-cho, Higashi-ku, Hamamatsu, Shizuoka, Japan
[d] Nagoya University Graduate School of Medicine, 1-1-20, Daikominami, Higashi-ku, Nagoya-shi, Aichi 461-8673, Japan

ARTICLE INFO

Available online 1 May 2014

Keywords:
Multi-Pixel Photon Counter
Gamma-rays
Gamma camera

ABSTRACT

We are developing a technique to fabricate fine spatial resolution (FWHM < 0.5 mm) and cost-effective photon counting detectors, by using silicon photomultipliers (SiPMs) coupled with a finely pixelated scintillator plate. Unlike traditional X-ray imagers that use a micro-columnar CsI(Tl) plate, we can pixelate various scintillation crystal plates more than 1 mm thick, and easily develop large-area, fine-pitch scintillator arrays with high precision. Coupling a fine pitch scintillator array with a SiPM array results in a compact, fast-response detector that is ideal for X-ray, gamma-ray, and charged particle detection as used in autoradiography, gamma cameras, and photon counting CTs. As the first step, we fabricated a 2-D, cerium-doped $Gd_3Al_2Ga_3O_{12}$ (Ce:GAGG) scintillator array of 0.25 mm pitch, by using a dicing saw to cut micro-grooves 50 μm wide into a 1.0 mm thick Ce:GAGG plate. The scintillator plate is optically coupled with a 3.0×3.0 mm pixel 4×4 SiPM array and read-out via the resistive charge-division network. Even when using this simple system as a gamma camera, we obtained excellent spatial resolution of 0.48 mm (FWHM) for 122 keV gamma-rays. We will present our plans to further improve the signal-to-noise ratio in the image, and also discuss a variety of possible applications in the near future.

1. Introduction

X-ray and gamma-ray imaging techniques are widely used in medicine, physics experiments and homeland security. As a conventional position sensitive scintillation detector, a scintillator array coupled to a position-sensitive photomultiplier tube (PSPMT) is commonly used in various applications. A paper published in 2004 [1] reported analysis of the spatial resolution based on Hamamatsu H8500 PMT coupled to different scintillation material arrays like CsI(Tl) and NaI(Tl). The paper suggests a good pixel identification with a position error of 400 μm as measured with 122 keV gamma rays. However, an actual spatial resolution of the camera is limited by the size of a scintillator pixel, hence ~1 mm for the NaI(Tl) used in the paper. Moreover, hygroscopicity of the NaI(Tl) and CsI(Tl) crystals as well as bulky, expensive PMTs prevents the detector to spread widely for various applications.

In contrast, high spatial resolution detector based on the columnar CsI(Tl) layer coupled to the EM-CCD through a fiber-optic plate is recently used as a flat panel detector for medical purposes. Recent research has demonstrated an excellent pixel resolution of 31–80 μm FWHM [2]. Despite its surprising image resolution, however, sensitivity to 59.5 keV gamma rays is only 23% due to a thin 70 μm columnar CsI(Tl) scintillator layer. While several photon-counting modes are proposed, energy resolution is also not good, typically ≥20% (FWHM) as measured with 122 keV gamma rays.

In this paper, we propose a concept of cost-effective scintillation detector array which realizes a moderate spatial resolution (0.48 mm FWHM) as well as good spectral resolutions (14% FWHM). In our approach, Ce-doped $Gd_3Al_2Ga_3O_{12}$ (Ce:GAGG) scintillator plate ($10 \times 10 \times 1$ mm^3) is cut using a dicing saw for micro-grooves to fabricate fine-pitch scintillator arrays. Note, Ce:GAGG is a brand-new scintillator featuring its high light yield, high density, fast decay time and mechanical stability [3]. Moreover, sensitivity of a 1-mm thick Ce:GAGG to 59.5 keV gamma rays is about 98%. To evaluate the performance of the fine-pitch scintillator array, we have developed a simple imaging detector based on the scintillator array and a silicon photomultiplier.

Particularly, the Multi-Pixel Photon Counter (MPPC), known as a kind of silicon photomultiplier family produced by Hamamatsu

* Corresponding author.
E-mail address: t_fujita@fuji.waseda.jp (T. Fujita).

http://dx.doi.org/10.1016/j.nima.2014.04.060
0168-9002/

Photonics K.K. [4,5], is a promising sensor for these purposes due to its high gain (10^5–10^6) comparable to that of PMTs, low bias supply (≤ 100 V), fast timing characteristics ($\simeq 50$ ns decay), and insensitivity to magnetic fields. In addition, silicon-based devices may be produced in large quantities as relatively low-cost devices. SiPMs are widely used in various fields such as medical applications, high energy physics, and environmental radiation monitoring [7,6,8]. In some research, SiPMs have been applied to the photo-detector of high spatial resolution detector [9,10].

This paper reports on our development of a simple imaging detector based on a fine-pitch scintillator array coupled to a large-area MPPC, and evaluates the performance of the detectors. We also investigate the limiting factors of spatial resolution and suggest the way to improve detector performance further.

2. Materials and methods

2.1. Fabrication of the scintillator array and detector formation

Conventionally, fine pixel scintillator arrays are fabricated by binding together pixels of scintillator crystals coated with a reflector, such as a mixture of powdered $BaSO_4$ and binders [11]. It is difficult to precisely fabricate a fine-pitch scintillator array whose pitch is smaller than 0.6 mm.

In our case, we fabricated a fine-pitch scintillator array as described below. We have processed a $10.0 \times 10.0 \times 1.0$-mm^3 scintillator plate. The scintillator plate is bonded with UV curing adhesive (PHOTOBOND300, SUNRISE MSI) to a $14.0 \times 14.0 \times 1.0$-mm^3 borosilicate glass plate. Thereafter the scintillator is carved to micro-grooves by using a dicing saw. The width of the micro-grooves is 50 μm and the depth is 900 μm. Each groove is coated with a mixture of powdered $BaSO_4$ and binders to limit the spread of scintillation photons from each pixel.

We fabricated a 0.25 mm pitch Ce:GAGG array in our method. Table 1 summarizes the basic characteristics of the Ce:GAGG scintillator and other scintillators [3,12]. The borosilicate glass

Table 1
Basic characteristics of scintillators.

Scintillator	Ce:GGAG	Ce:LYSO	CsI(Tl)
Density [g/cm^3]	6.63	7.10	4.51
Light yield [ph/MeV]	42 000	25 000	66 000
Decay time [ns]	52.8 (73%) and 282 (27%)	40	800–6000
Peak wavelength [nm]	520	420	550

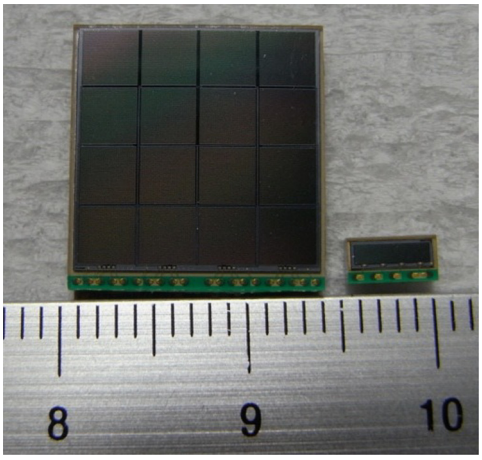

Fig. 2. Photo of MPPC arrays (Left: S11830-3344MB, Right: S10984-050P, Hamamatsu Photonics K.K.).

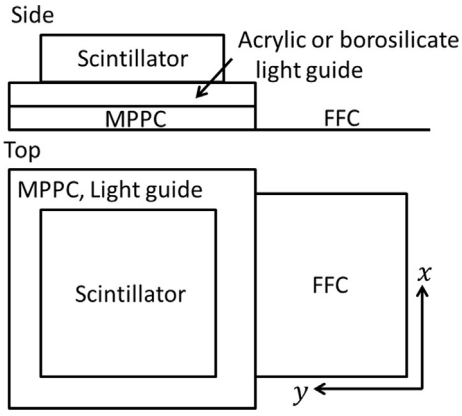

Fig. 3. The schematic side and top view of the detector.

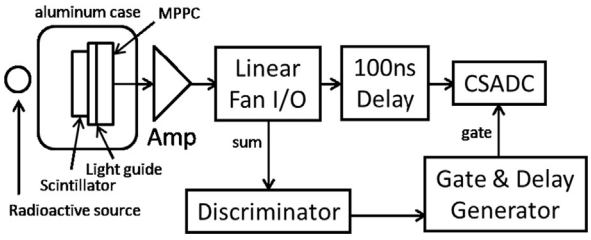

Fig. 4. Diagram of the readout system of the measurements.

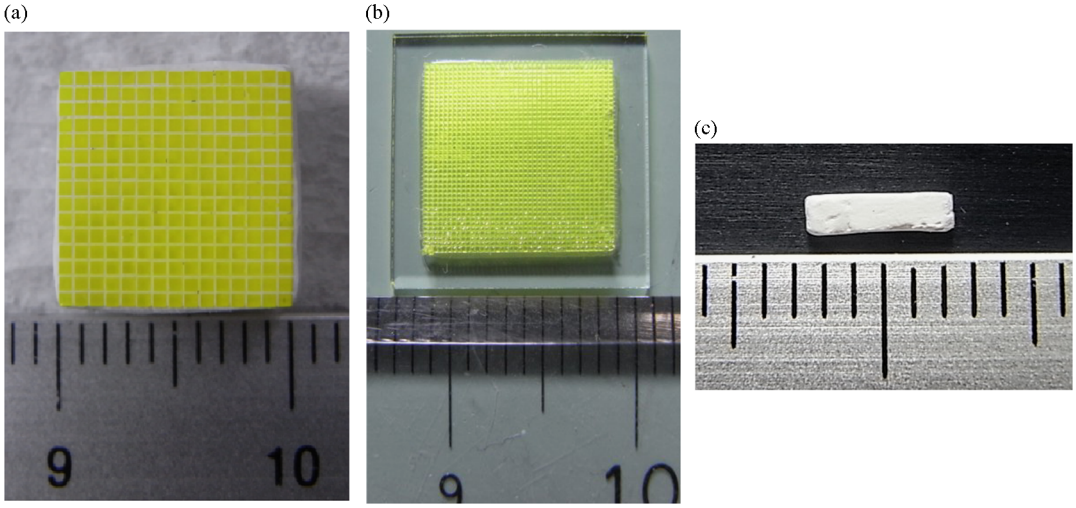

Fig. 1. Photo of scintillator arrays, (a) 0.60-mm pitch Ce:GAGG array, (b) 0.25-mm pitch Ce:GAGG array and (c) 1-D Ce:LYSO array.

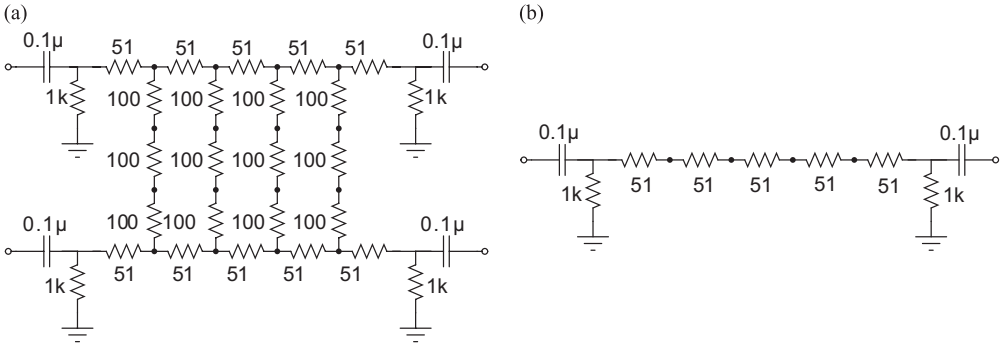

Fig. 5. (a) 2-D and (b) 1-D resistive charge division network circuits.

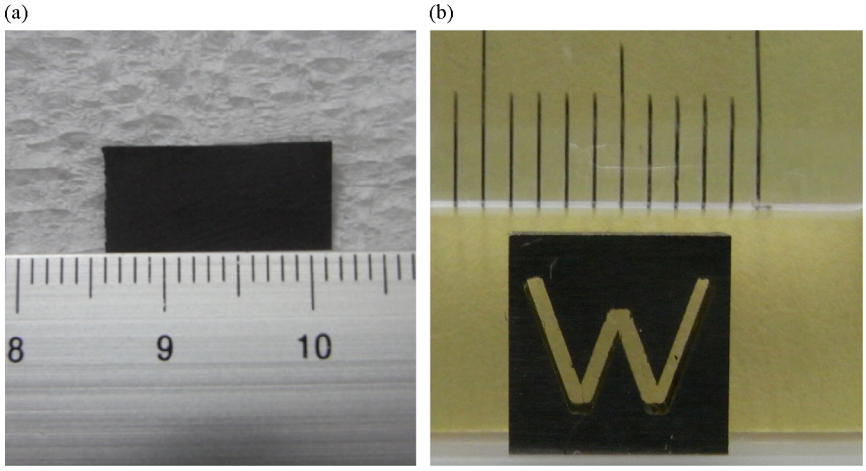

Fig. 6. Photo of (a) the thin tungsten sheet and (b) the tungsten collimator.

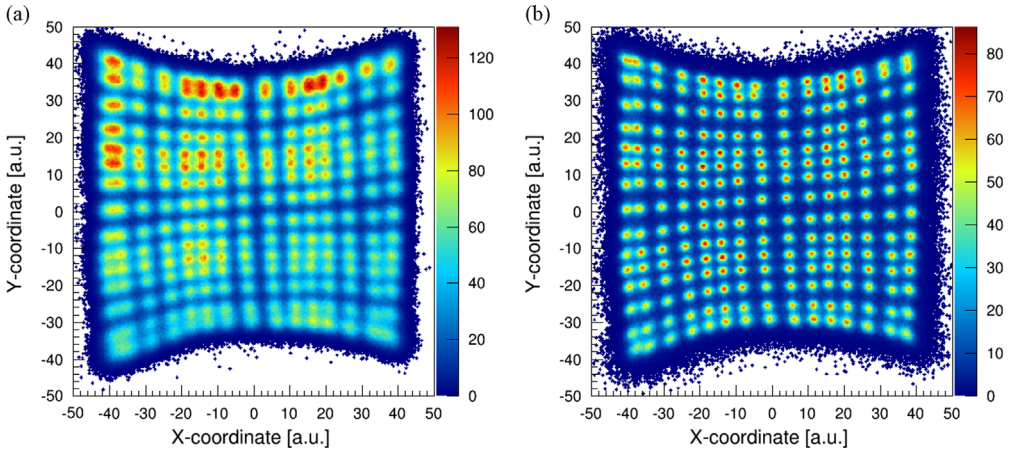

Fig. 7. Flood maps of 0.60-mm pitch Ce:GAGG array irradiated by (a) ^{241}Am and (b) ^{57}Co sources.

bonded to the 0.25 mm pitch array takes a role of a light guide. For comparison, we fabricated a 0.60 mm pitch Ce:GAGG array in the conventional way. The 0.60 mm pitch array is coupled with an acrylic light guide 1.0 mm thick using silicon optical grease (OKEN 6262A). The volume of a pixel of 0.60 mm pitch Ce:GAGG array is $0.50 \times 0.50 \times 5.0\ \mathrm{mm}^3$ and each pixel is divided by a 0.1-mm reflective $BaSO_4$ layer. These scintillator arrays are shown in Fig. 1.

These scintillator arrays are coupled to a 4×4 MPPC array (S11830-3344MB, Hamamatsu Photonics K.K.) using the silicon optical grease. The MPPC array is shown in Fig. 2. Each pixel of the MPPC array has a photosensitive area of $3.0 \times 3.0\ \mathrm{mm}^2$, and is composed of Geiger-mode APDs arranged at a pitch of 50 μm. A schematic side and top view of the detector is shown in Fig. 3

In addition to experiments conducted to evaluate the performance of the detectors, we evaluated the effect of macro-pixel sizes of MPPC arrays on the pixel resolution. We used a 1×2 pixel Ce:LYSO scintillator array as shown in Fig. 1(c). The volume of each pixel is $0.50 \times 0.50 \times 5.0\ \mathrm{mm}^3$ and the two pixels are divided with a 0.1-mm thick reflective $BaSO_4$ layer. The Ce:LYSO array was coupled to two different types of MPPC arrays by using optical grease. One is the $3.0 \times 3.0\ \mathrm{mm}^2$-pixel MPPC array (S11830-3344MB, Hamamatsu Photonics K.K.). The other is a $1.0 \times 1.0\ \mathrm{mm}^2$-pixel MPPC array (S10984-050P, Hamamatsu Photonics K.K.). These MPPC arrays are shown in

Fig. 2. The Ce:LYSO array was coupled to the 3.0×3.0 mm^2-pixel MPPC array through the acrylic light guide. On the other hand, the Ce:LYSO array is coupled directly to 1.0×1.0 mm^2-pixel MPPC array.

2.2. Experimental setup

To evaluate performance of the detectors, we performed three different measurements as described in detail below. In these experiments, the MPPC arrays are operated at a gain of 7.5×10^5. Fig. 4 shows a diagram of the setup in these experiments. To reduce the number of output signals from the MPPC array, we applied a charge division readout technique [6,13]. In these experiments, a 2-D resistive charge division network in Fig. 5 was used to compile the 16 signals output from the MPPC array into four position-encoded analog signals.

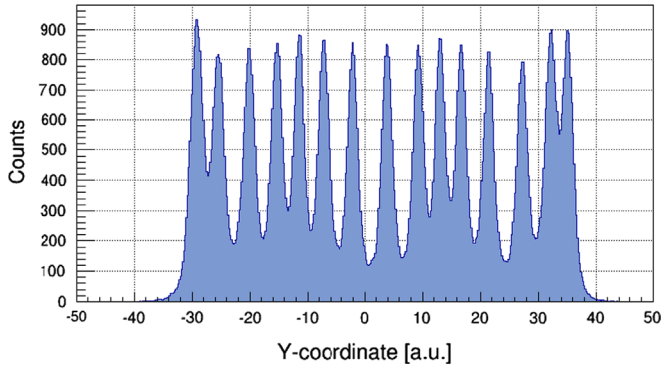

Fig. 8. The projection to *y*-axis of the scintillator pixels in tenth column from the left in the flood map of the 0.60 mm pitch array irradiated by ^{57}Co.

These signals are amplified with a wideband amplifier (Phillips Scientific Model 6954-B-10) and sent to a linear fan I/O module (Phillips Scientific Model 740) in order to sum the signals for triggering. Each signal is delayed with a 100 ns delay circuit (Technoland N-TS 100) and is fed into the charge sensitive ADC (HOSHIN V005). The sum of signals is fed into a discriminator (Technoland N-TM 405). Thereafter the discriminator outputs a trigger signal. The trigger signal is sent to a gate and delay generator (Technoland N-TM 307) to create a gate signal 750-ns wide. Thereafter the gate signal is fed into the charge sensitive ADC.

In measurement of flood maps and energy spectra, the detectors covered with no collimator are irradiated by radioactive gamma-ray sources from a distance of 5.0 cm. In order to measure the spatial resolution of the detectors, the half area of each detectors was covered with a 0.5-mm thick thin tungsten sheet shown in Fig. 6. Spatial resolution was determined by an average of FWHMs of the line spread functions calculated from fitting curves of edge spread function slices. In the imaging tests, a W-type tungsten collimator was placed on the detectors. In spatial resolution measurements and imaging tests, the sensitivity of pixels calculated from flood maps was used to compensate for the measured counts of each scintillator pixel.

To evaluate the effect of the size of MPPC array macro-pixels on the pixel resolution, we measured the pixel resolution of the Ce:LYSO 1-D array coupled to the MPPC arrays. The block diagram of the experimental setup was the same as the one described before.

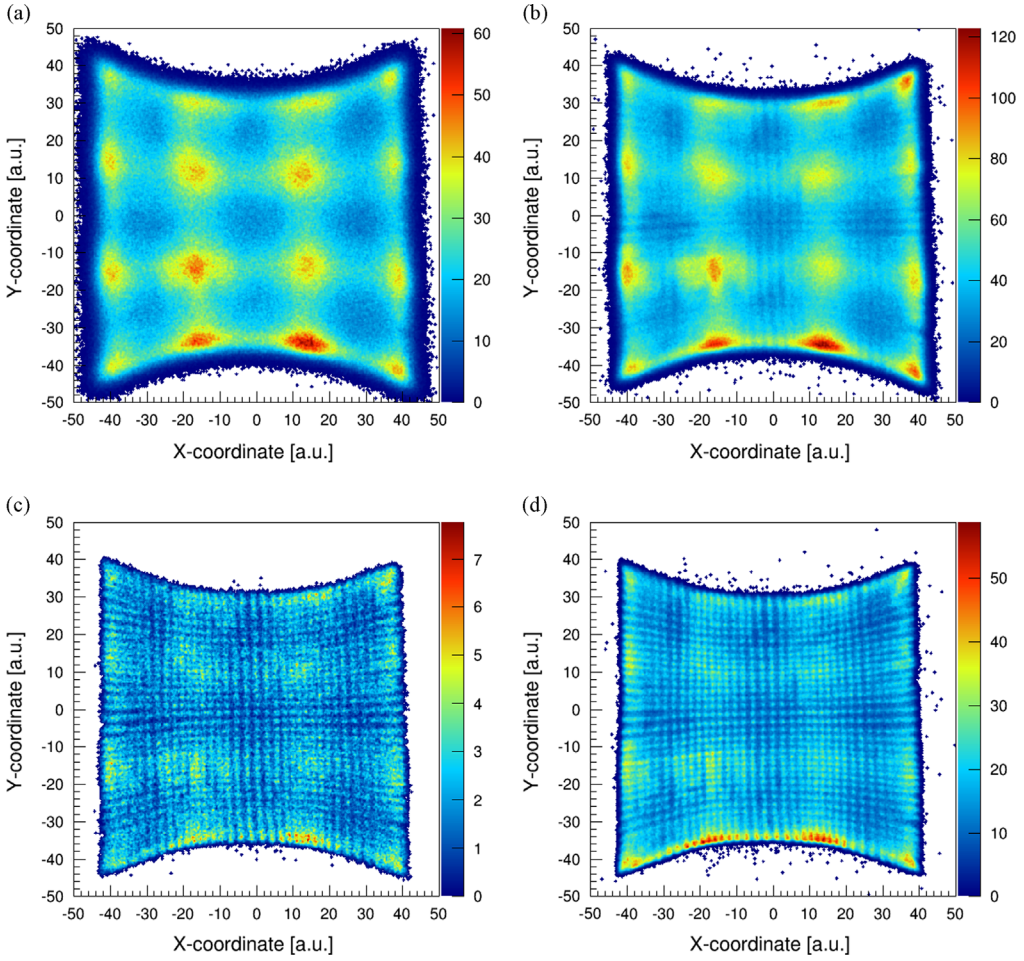

Fig. 9. Flood maps of 0.25-mm pitch Ce:GAGG array irradiated by (a) ^{241}Am, (b) ^{57}Co, (c) ^{133}Ba, and (d) ^{60}Co sources.

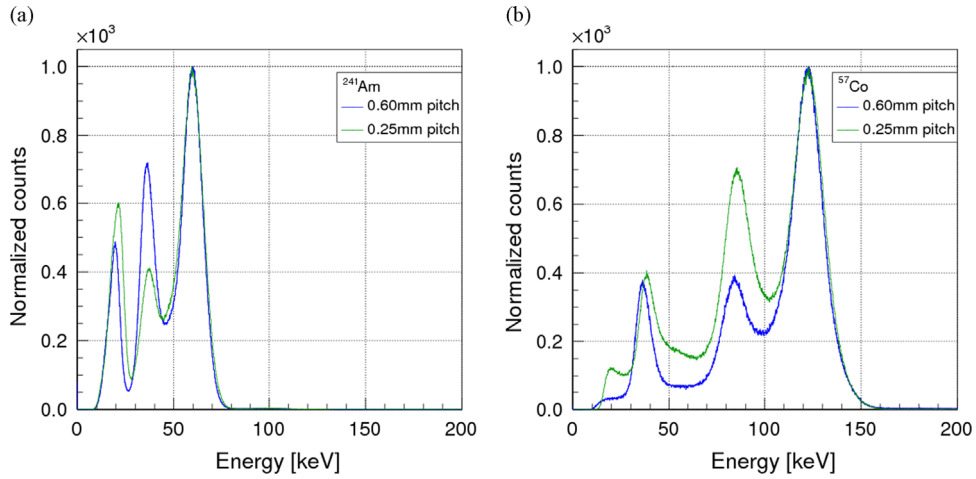

Fig. 10. Energy spectra of (a) ^{241}Am and (b) ^{57}Co sources. (a) ^{241}Am, (b) ^{57}Co

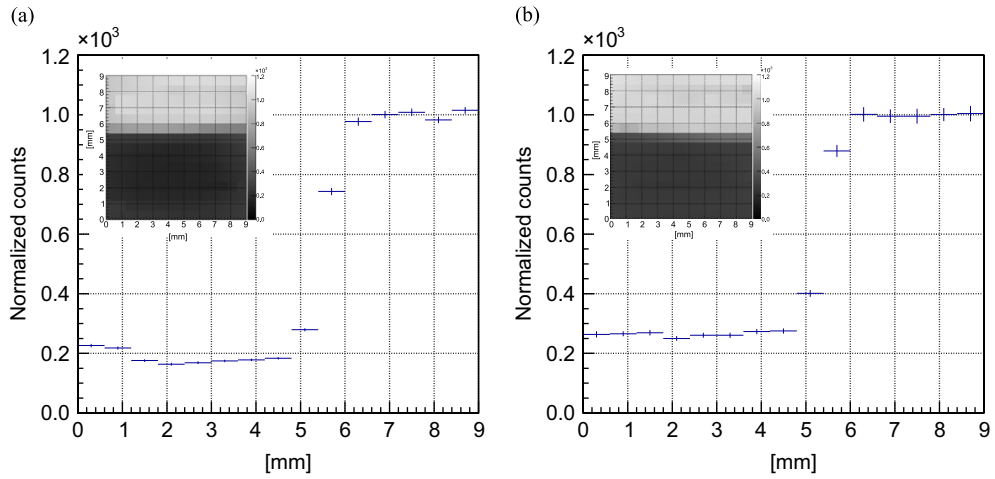

Fig. 11. Edge spread functions of 0.60-mm pitch Ce:GAGG array. Spatial resolution was 0.88 ± 0.07 mm (FWHM) at 59.5 keV and 0.77 ± 0.09 (FWHM) at 122 keV. (a) 59.5 keV, (b) 122 keV.

The resistive charge division network was changed to a 1-D resistive charge division network circuit. The Ce:LYSO array was placed at the center of a macro-pixel of MPPC arrays. The pixel resolution was converted into units of mm according to the true pixel pitch of the Ce:LYSO array.

3. Results

3.1. Performance of the detector

Fig. 7 shows the flood maps of the 0.60 mm pitch array irradiated by (a) ^{241}Am and (b) ^{57}Co sources. Each pixel is successfully resolved at 122 keV of the ^{57}Co. Fig. 8 shows the projection to *y*-axis of the scintillator pixels in tenth column from the left in the flood map of the 0.60 mm pitch array irradiated by ^{57}Co. The average pixel resolution was 0.34 mm FWHM. In addition, the best and worst pixel resolution was respectively 0.25 mm FWHM and 0.43 mm FWHM.

Fig. 9 shows the flood maps of the 0.25 mm pitch array irradiated by (a) ^{241}Am, (b) ^{57}Co, (c) ^{133}Ba, and (d) ^{60}Co sources. Although each pixel was not able to be resolved at 122 keV of the ^{57}Co source, most of the pixels were able to be resolved at higher energy than 356 keV of the ^{133}Ba source. The regions of the flood maps corresponding to the pixels of the 0.25-mm pitch Ce:GAGG array were determined with the flood map of the array irradiated by the ^{60}Co source, and 30×30 pixels of the array are used in other measurements.

Energy spectra of gamma-rays from (a) ^{241}Am and (b) ^{57}Co sources are shown in Fig. 10. The 0.60-mm pitch array showed an energy resolution of 22% FWHM at 59.5 keV and 13% FWHM at 122 keV. On the other hand, energy resolution of the 0.25-mm pitch array was 24% FWHM at 59.5 keV and 14% FWHM at 122 keV. The deterioration of energy resolution seems to be caused by the overlap of pixels in the flood map. To quantify the effect of the pixel overlap on the deterioration of resolution, we need additional experiments using a ~ 0.2 mm diameter pinhole collimator.

Fig. 11 shows the results of edge spread function measurement with the 0.60-mm pitch Ce:GAGG array at the energy of (a) 59.5 keV and (b) 122 keV. Spatial resolution was 0.88 ± 0.07 mm (FWHM) at 59.5 keV and 0.77 ± 0.09 mm (FWHM) at 122 keV. Fig. 12 shows the edge spread functions of the 0.25-mm pitch Ce:GAGG array. Spatial resolution was 0.69 ± 0.05 mm (FWHM) at 59.5 keV and 0.48 ± 0.05 mm (FWHM) at 122 keV.

Figs. 13 and 14 show the results of imaging tests of the detectors at the energy of (a) 59.5 keV and (b) 122 keV. In com-

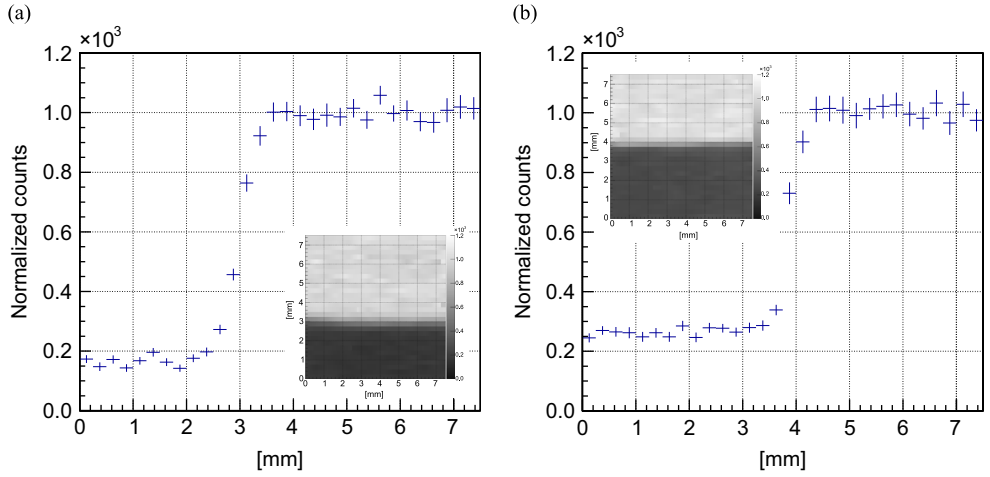

Fig. 12. Edge spread function of 0.25-mm pitch Ce:GAGG array. Spatial resolution was 0.69 ± 0.05 (FWHM) at 59.5 keV and 0.48 ± 0.05 (FWHM) at 122 keV. (a) 59.5 keV, (b) 122 keV

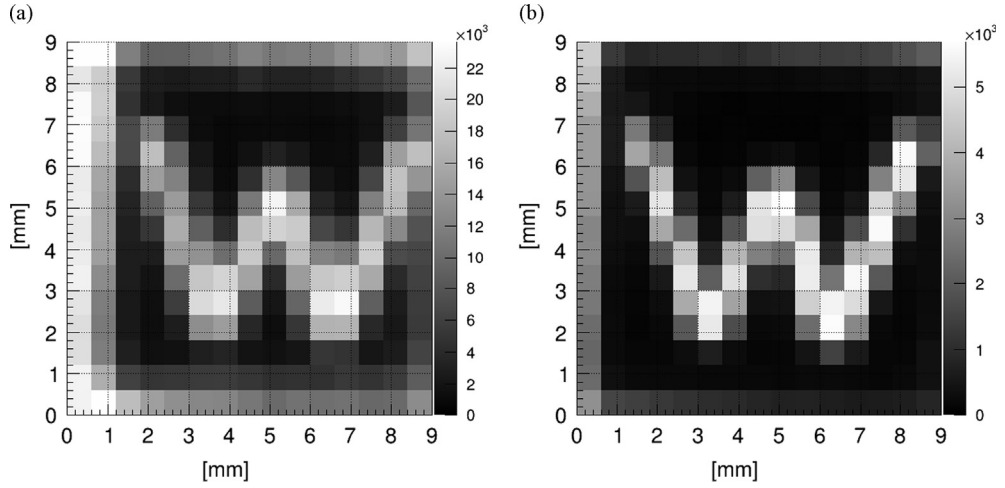

Fig. 13. Results of imaging tests with 0.60-mm pitch Ce:GAGG array. (a) 59.5 keV, (b) 122 keV.

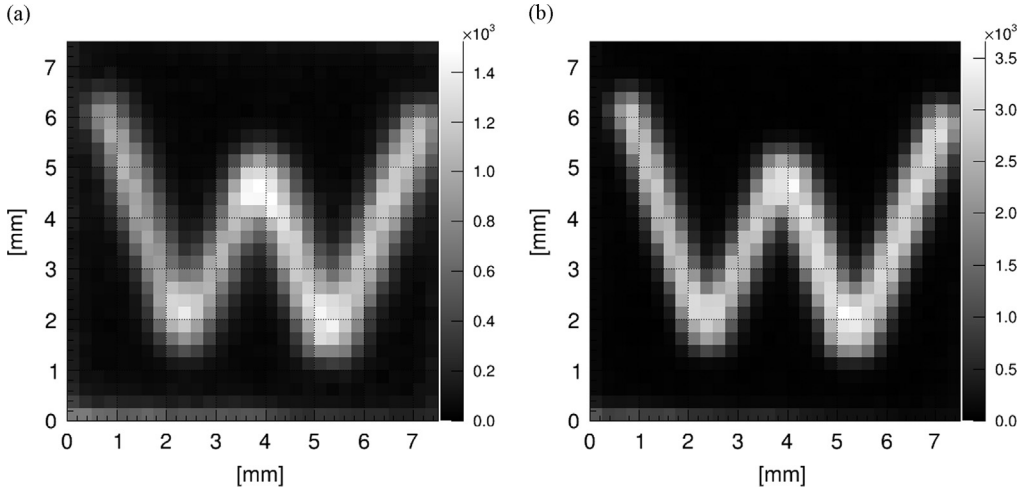

Fig. 14. Results of imaging tests with 0.25-mm pitch Ce:GAGG array. (a) 59.5 keV, (b) 122 keV.

parison with the images in Fig. 13, the images in Fig. 14 were significantly improved. This is because the sampling period of the 0.25 mm pitch array is shorter than the sampling period of the 0.60 pitch array. Compared with the image in Fig. 14(a), the image in Fig. 14(b) is sharper. The improvement of the pixel resolution has led to this improvement.

3.2. Comparison of the pixel resolution of MPPC array

Fig. 15 compares the reconstructed position distributions of the 0.60-mm pitch Ce:LYSO scintillator array coupled to 1.0 × 1.0-mm^2 pixel MPPC array and 3.0 × 3.0-mm^2 pixel MPPC array at an energy of 122 keV of the ^{57}Co source and 356 keV of the ^{133}Ba source. The pixel

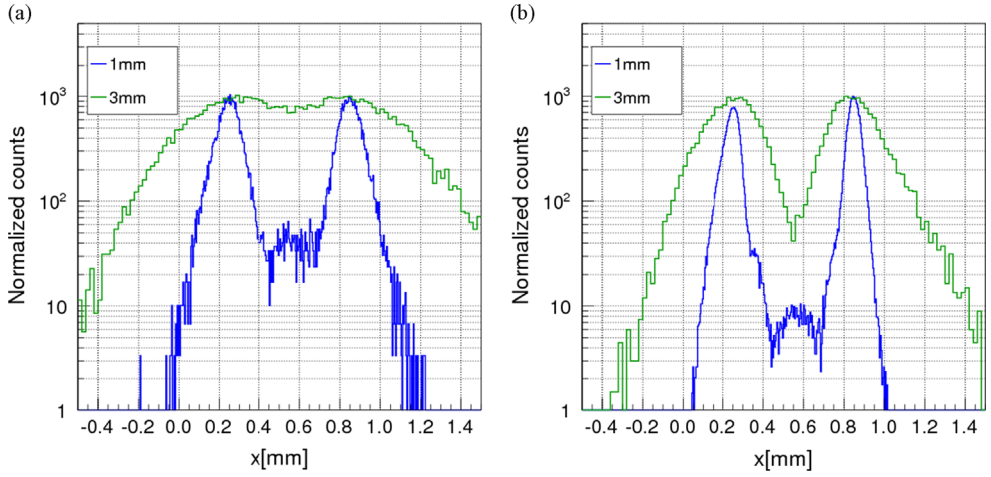

Fig. 15. The pixel resolution of the 1.0×1.0 mm^2 pixel and 3.0×3.0 mm^2 pixel MPPC arrays (a) at 122 keV and (b) at 356 keV.

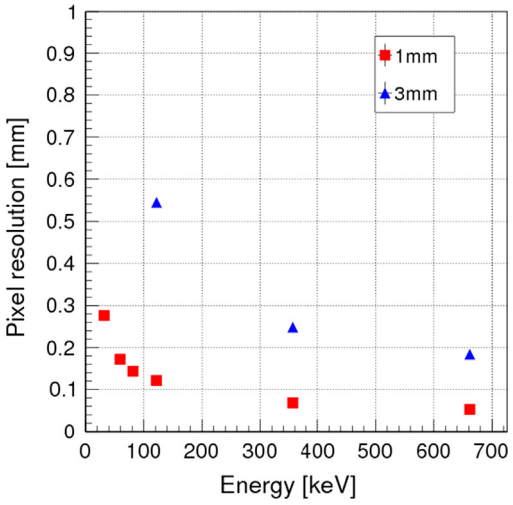

Fig. 16. Energy dependency of pixel resolution.

resolution of the 1.0×1.0-mm^2 pixel MPPC array was 0.11 ± 0.01 mm (FWHM) at 122 keV and 79 ± 5 μm (FWHM) at 356 keV. That of the 3.0×3.0-mm^2 pixel MPPC array was 0.58 ± 0.02 mm (FWHM) at 122 keV and 0.31 ± 0.01 mm (FWHM) at 356 keV, respectively. The pixel resolution of the 1.0×1.0-mm^2 pixel MPPC array is dramatically improved as compared to that of the 3.0×3.0-mm^2 pixel MPPC array.

Fig. 16 summarizes the energy dependency of pixel resolution of the Ce:LYSO array coupled to respective MPPC arrays. The 1.0×1.0-mm^2 pixel MPPC array coupled to the Ce:LYSO array showed exceedingly high pixel resolution. And even at low energy of 59.5 keV, the pixel resolution was 0.17 mm FWHM, which offers sufficient performance to clearly resolve pixels of a 0.25-mm pitch Ce:LYSO scintillator array.

4. Conclusion

This paper reports on a 0.25-mm pitch Ce:GAGG scintillator array that we fabricated by using a dicing saw to cut micro-grooves 50-μm wide, and evaluated the performance of a simple imaging detector based on the scintillator array and large-area 3.0×3.0-mm^2 pixel MPPC array readout using a resistive charge division readout technique. Even when using this simple system as a gamma camera, the detector showed a spatial resolution of 0.48 ± 0.05 mm FWHM and an energy resolution of 14% FWHM at 122 keV. According to flood maps of the detectors irradiated by respective gamma-ray sources, the overlap of pixels in flood maps seems to cause the deterioration of detector performance. Higher performance is expected by improving pixel resolution of the detector. According to a comparison of pixel resolution of MPPC arrays having different pixel sizes, we can state that the detector's pixel resolution is limited by the size of pixels of MPPC array. The 0.60-mm pitch Ce:LYSO scintillator array coupled to the 1.0×1.0-mm^2 pixel MPPC array showed a high pixel resolution of 0.17 mm FWHM even at a low energy of 59.5 keV, and was sufficient to resolve 0.25 mm pitch Ce:LYSO scintillator pixels. Since the Ce:GAGG scintillator has a higher light yield than the Ce:LYSO scintillator, a 0.25-mm pitch Ce:GAGG scintillator array coupled to the 1.0×1.0-mm^2 pixel MPPC array is expected to show higher performance. Moreover, we would say that a maximum count rate of our detector should be $>$ MHz, because the output signal from the MPPC coupled with a Ce:GAGG scintillator has quite fast decay time of $\sim$100 ns. We should perform more careful and detailed follow-up experiments to evaluate limiting conditions, such as maximum count rate, crosstalk between pixels, max intensity, and oversaturation problems. Further we will develop a large-area 1.0×1.0-mm^2 pixel MPPC array and report on an improved imaging detector in the near future. We will present a variety of possible applications, such as a spectral CT, medical pin-hole gamma camera, and alpha camera.

References

[1] R. Pani, et al., Nuclear Instruments and Methods in Physics Research Section A 527 (2004) 54.
[2] David J. Hall, et al., Nuclear Instruments and Methods in Physics Research Section A 678 (2012) 64.
[3] Kei Kamada, et al., Journal of Crystal Growth 352 (2012) 88.
[4] K. Yamamoto, et al., IEEE Nuclear Science Symposium Conference Record 2 (2007) 1511.
[5] K. Sato, et al., IEEE Nuclear Science Symposium Conference Record NSS/MIC (2010), p. 243.
[6] T. Kato, et al., Nuclear Instruments and Methods in Physics Research Section A 699 (2013) 235.
[7] J. Kataoka, et al., Nuclear Instruments and Methods in Physics Research Section A 732 (2013) 403.
[8] M. Danilov, Nuclear Instruments and Methods in Physics Research Section A 581 (2007) 451.
[9] H. Sabet, et al., IEEE Transactions on Nuclear Science NS-59 (2012) 1841.
[10] H. Sabet, et al., IEEE Transactions on Nuclear Science NS-60 (2013) 1000.
[11] T. Kato, et al., Nuclear Instruments and Methods in Physics Research Section A 638 (2011) 83.
[12] I.G. Valais, et al., Nuclear Instruments and Methods in Physics Research Section A 569 (2006) 201.
[13] S. Siegel, et al., IEEE Transactions on Nuclear Science NS-43 (1996) 1634.